Global Changes in Drought Conditions under Different Levels of Warming

G. Naumann[1], L. Alfieri[1], K. Wyser[2], L. Mentaschi[1], R. A. Betts[3, 4], H. Carrao[1], J. Spinoni[1], J. Vogt[1], and L. Feyen[1]

[1]European Commission, Joint Research Centre, Ispra, Italy

[2]Swedish Meteorological and Hydrological Institute, Rossby Centre, Norrköping, Sweden

[3]Met Office Hadley Centre, Exeter, UK

[4] College of Life and Environmental Sciences, University of Exeter, UK

Corresponding author: Gustavo Naumann (gustavo.naumann@ec.europa.eu)

Key points

- This paper proposes a methodology for assessing global changes in drought characteristics under different warming levels, including an assessment of the related uncertainties.
- Drought magnitude will halve in 20% of the global land surface with warming of 1.5°C and higher levels.
- A progressive and significant increase in frequency of droughts is projected with warming in the Mediterranean basin, most of Africa, West and Southern Asia, Central America and Oceania, where droughts are projected to happen 5 to 10 times more frequent even under ambitious mitigation targets.

This article has been accepted for publication and undergone full peer review but has not been through the copyediting, typesetting, pagination and proofreading process which may lead to differences between this version and the Version of Record. Please cite this article as doi: 10.1002/2017GL076521

Abstract. Higher evaporative demands and more frequent and persistent dry spells associated with rising temperatures suggest that drought conditions could worsen in many regions of the world. In this study, we assess how drought conditions may develop across the globe for 1.5, 2, and 3°C warming compared to pre-industrial temperatures. Results show that 2/3 of global population will experience a progressive increase in drought conditions with warming. For drying areas, drought duration are projected to rise at rapidly increasing rates with warming, averaged globally from 2.0 month/°C below 1.5°C to 4.2 month/°C when approaching 3°C. Drought magnitudes could double for 30% of global land mass under stringent mitigation. If contemporary warming rates continue, water supply-demand deficits could become five-fold in size for most of Africa, Australia, southern Europe, southern and central states of the US, Central America, the Caribbean, north-west China and parts of Southern America. In approximately 20% of the global land surface, drought magnitude will halve with warming of 1.5°C and higher levels, mainly most land areas north of latitude 55°N, but also parts of South-America, Eastern and South-eastern Asia. A progressive and significant increase in frequency of droughts is projected with warming in the Mediterranean basin, most of Africa, West and Southern Asia, Central America and Oceania, where droughts are projected to happen 5 to 10 times more frequent even under ambitious mitigation targets and current 100 year events could occur every 2 to 5 years under 3°C of warming.

Plain Language Summary

This research investigates the climatology of global drought conditions under different global warming levels. We consider warming levels of 1.5{degree sign}C and 2{degree sign}C set out as mitigation targets in the Paris Agreement, as well as 3{degree sign}C that is closer to what is expected by the end of the 21st Century if current emissions trends are retained.We found that the magnitude of droughts is likely to double in 30% of the global land mass under stringent mitigation policies. If global warming continues at the present rate, water supply-demand deficits would increase five-fold while current 1-in-100 year droughts would occur every 2 to 5 years for most of Africa, Australia, southern Europe, southern and central USA, Central America, the Caribbean, north-west China and parts of Southern America. Approximately two thirds of the global population will experience a progressive increase in drought hazard with warming. In drying areas, drought durations are projected to rise rapidly with warming. The main impacts of long lasting droughts are linked to the lowering of the groundwater and of the water levels in reservoirs. This will impede replenishment of water supplies and may result in a difficult recovery and prolonged socio-economic impacts after severe droughts.

1. Introduction

Drought is a climatic hazard that occurs in most world climates and can have considerable economical, societal and environmental impacts. While global long-term trends in drought frequency and severity remain an element of debate in the literature (Dai 2013; Sheffield *et al.*, 2012; Trenberth *et al.*, 2014), in part owing to a lack of observations and a long list of sometimes conflicting drought definitions, regional studies suggest an increasing trend in the intensity and frequency of droughts in several parts of the world, such as the Mediterranean (Spinoni *et al.*, 2015a, Vicente Serrano *et al.*,

2014), West Africa (Dai 2013; Sheffield *et al.*, 2012, Masih *et al.*, 2014), and Central China (Wang *et al.*, 2017). In other regions, such as central North America (Peterson *et al.*, 2013) and north-west Australia (Jones *et al.*, 2009), drought conditions have become less severe in the second half of the 20th century.

Alterations in surface hydroclimatic conditions due to climate change are complex, yet decreasing regional precipitation, more intense and frequent dry spells, and increasing evaporative demands driven by global warming could considerably worsen droughts in many regions of the globe. This understanding in combination with the devastating impacts of droughts on society has recently resulted in a number of global assessments of future drought conditions (e.g., Burke & Brown 2008; Sheffield & Wood 2008; Orlowsky & Seneviratne, 2013, Taylor *et al.*, 2013; Prudhomme *et al.*, 2014; Touma *et al.*, 2015, Wanders *et al.*, 2015, Zhao & Dai 2015; Zhao & Dai 2016).

Projections of the evolution of droughts under global warming vary depending on the drought indices adopted. Due to its complexity and the diverse interests of those investigating droughts, no universal definition of droughts exists (Lloyd-Hughes, 2014). A drought can generally be defined as an extended period of abnormal below average natural water availability. Because droughts mostly arise from a significant deficiency in moisture supply in form of precipitation, many studies have focused on the input side, for example through the use of the Standard Precipitation Index (SPI; McKee *et al.*, 1993). Yet, high evaporative losses can seriously alter natural water availability, which has led to the use of water-balance methods such as the Palmer Drought Severity Index (PDSI; Palmer 1965) and the Standardized Precipitation Evapotranspiration Index (SPEI; Vicente-Serrano *et al.*, 2010). Using these two indices, Cook et al. (2014) show that an increased atmospheric evaporative demand (AED) due to warming not only intensifies drying in areas where precipitation will reduce, but that it will also drive areas into drought that will experience little drying or even wetting from precipitation trends alone. Hence, especially in view of global warming, accounting for alterations in atmospheric demand due to changes in specific humidity, surface wind speed, and surface down welling short- and long-wave radiation is essential to portray the evolution of droughts in a warmer world. However, these processes are complex and depend on the different sensitivity of the drought indices to the atmospheric evaporative demand as a function of climate characteristics (Vicente-Serrano et al., 2015). For instance, an AED increase in areas of abundant precipitation might not increase drying (since temporal variability of precipitation is much higher than the variability of AED and droughts mostly depend on precipitation), and could even favor vegetation activity and growth given that water availability is not a limiting factor and vegetation growth is more constrained by temperature and radiation.

The metric used here (SPEI) does not account for the physiological effects of elevated CO_2 (eCO_2) on transpiration, which can be very important (Betts *et al.*, 2007). Decreasing stomatal conductance

induced by eCO2 increases canopy water-use efficiency (hence lower transpiration rates per unit leaf), yet this mechanism is potentially offset by the enhancement of leaf area and rooting depth (Donohue *et al.,* 2017). Predicted responses of transpiration to eCO2 are highly variable amongst process-based models depending on what processes are accounted for and their parametrization, highlighting the current uncertainty about plant water use in response to eCO2 (De Kauwe *et al.,* 2013). Recent findings further suggest that land surface models show systematic bias in simulating water and energy fluxes under water-stressed conditions (Ukkola *et al.,* 2016). Due to the large uncertainty in the estimation of evapotranspiration that takes into account the effect of eCO2 and the consequent warming we build our analysis on reference evapotranspiration (ETo), which is a supply-independent measure of the evaporative demand of a terrestrial climate and represents the rate at which a given climate is trying to evaporate water from the soil-vegetation system (Scheff & Frierson 2014). ETo only depends on the meteorological inputs and it has the advantage of being spatially comparable under different climates and environmental conditions (Beguería et al., 2014). For instance, Feng et al. (2017) shows that drought indices normalized with reference evapotranspiration (Penman-Monteith) show comparable dryness to the soil moisture in the US, while empirical estimations (Thornthwaite) shows more unrealistic estimations. Moreover, the authors show that the drought indices that includes Penman-Monteith estimations are closely related to soil moisture both during the baseline period and for the CMIP5 projections.

Assessments of future droughts also strongly depend on the greenhouse gas emissions scenario, the time horizon, and the set of climate simulations analyzed (Zhao & Dai, 2016). Previous assessments for selected scenarios and time windows provide valuable information in that they depict the evolution of the future drought hazard across the globe for the chosen scenario and time period. Yet, they do not directly link the frequency and severity of droughts to different thresholds of warming. Understanding the benefits of curbing global warming is, however, essential to support the Paris goals to keep warming below 2°C compared to pre-industrial temperatures and pursue a tougher target of 1.5°C (UNEP, 2016).

Here we present the first assessment of the climatology of drought conditions across the world under different levels of global warming. We consider Specific Warming Levels (SWLs) of 1.5°C and 2°C set out as mitigation targets in the Paris Agreement, as well as 3°C that is closer to what would be expected by the end of 21st Century if current emissions pledges (Nationally Determined Contributions, NDCs) are followed (Raftery *et al.*, 2017). Our analysis is based on the Representative Concentration Pathways (RCP) of 8.5 W m^{-2} as it allows to consider the full range of SWLs using a consistent set of projections, whereas lower emission pathway scenarios (RCP 2.6 and RCP 4.5) typically do not reach higher levels of warming (James *et al.*, 2017). This assumes that the drought

climatology is fully defined by the SWL and not by the pathway to arrive to it. Maule *et al.* (2017) recently showed that the effect of different concentration pathways is small compared to internal climate variability on the timescales involved in reaching +2°C of warming.

We use an ensemble of high-resolution climate simulations from downscaled General Circulation Models (GCMs) under RCP 8.5 and analyze drought conditions over 30-year time windows centered on the SWLs. The set of climate models were selected as representative of a range of outcomes for future climate change, including high and low climate sensitivity, different biases in baseline precipitation climatology, and different global patterns of precipitation change (Alfieri et al., 2017; 2018). Drought changes with respect to historical conditions are derived from a peak over threshold analysis using the SPEI multi-scalar drought index that represents both the supply and demand sides of the surface moisture balance. Results are aggregated by region and global land surface, while the agreement of the ensemble projections is assessed through dedicated statistics. Section 2 presents the methodological aspects of our approach. Key results are then described in Section 3, followed by a discussion and concluding remarks in Section 4.

2. Data and methods

The analysis is based on a set of seven climate projections under the concentration pathway scenario RCP8.5 produced with EC-EARTH3-HR v3.1 (Hazeleger *et al.,* 2012; Alfieri *et al.,* 2017) by the Swedish Meteorological and Hydrological Institute (SMHI). The RCP 8.5 scenario assumes a CO_2 equivalent of about 1370 ppm and a corresponding warming of approximately 4.0°C with respect to pre-industrial temperatures by the end of the 21st century (van Vuuren *et al.,* 2011), which allows evaluating climate change effects under low as well as high levels of warming. Downscaled projections were obtained by forcing EC-EARTH3-HR with Sea Surface Temperature (SST) and sea-ice concentrations from an independent set of driving GCMs produced within the Coupled Model Intercomparison Project Phase 5 (CMIP5) as listed in Table S1. The seven forcing datasets were selected to represent the full spectra of all CMIP5 models by taking the models that have high or low climate sensitivity (IPSL-CM5A-LR and GFDL-ESM2M), or show extreme wet or dry response (GISS-E2-H and IPSL-CM5A-MR) at a given warming level. Together with the other three simulations, the seven members form an ensemble that covers the full width of the climate response in the CMIP5 database and thereby addresses the uncertainty in the climate projections. The benefits of downscaling the model outputs with EC-EARTH3-HR are to render uniform the simulations and increase their spatial resolution from the different original grids to 0.35°, leading to an improved characterization of drivers of the hydrological cycle (Demory *et al.,* 2014) and comparable statistics among the models. Raw climate outputs rather than bias-corrected data were used to ensure conservation principles and physical consistency between the atmospheric variables, to avoid effects

of data quality and resolution in global observational datasets, and to exclude inflation of the magnitude of relative trends in precipitation extremes induced by bias correction (Ehret *et al.,* 2012; Themeßl *et al.,* 2012; Huang et al., 2014; Cannon *et al.,* 2015). The procedure to compute the drought indicator (SPEI) involves the standardization of the difference between precipitation and reference evapotranspiration (ETo) by means of their monthly distributions. This procedure acts as an indirect bias correction of all the relevant variables as the final results are based on the standardized values and droughts are defined by dimensionless thresholds that correspond to specific probability values.
The average global warming from the pre-industrial era is 0.6°C at the end of the baseline calculated from the 21-year running mean of the annual observed near surface temperature (GISTEMP Team, 2017) averaged over the globe. In order to define the year of passing the SWLs for each climate ensemble member we added the change in projected global warming since 2005 to the observed warming in 2005, with the change based on the 21-year running mean of the global average temperature derived from the raw climate data. The resulting years of passing the SWLs are listed in Table S1.

Our analyses are based on the Standardized Precipitation-Evaporation Index (SPEI; Vicente-Serrano *et al.,* 2010), a standardized drought indicator (i.e. with mean=0 and standard deviation=1) that represents different features of the water balance and therefore is also sensitive to the variability and changes in climatic variables other than precipitation. Similar to the PDSI it includes the effects of the reference evapotranspiration on drought severity, yet it has the advantage of aggregating variables over different time dimensions that allows identifying different drought types and impacts, similar to the SPI (Beguería *et al.,* 2014). Recent studies evaluated linkages between the accumulation period of drought indicators and impacts in various sectors based on empirical data (Sepulcre-Cantó *et al.,* 2012; Trambauer *et al.,* 2014; Naumann *et al.,* 2015; Bachmair *et al.,* 2016; Blauhut *et al.,* 2016). These indicate that dependencies between drought predictors and impacts are sector- and region-specific. However, a 12-month aggregation period provides a good summary of the annual drought conditions and is useful for several purposes. For instance, Blauhut et al., (2016) show that SPEI with a 12-month accumulation period is the overall best predictor of the likelihood of impact occurrence in different sectors and macro regions in Europe. We therefore present changes in drought hazard based on the latter, further referred to as SPEI-12. This implies focusing on longer-term water deficits, representing hydrological droughts with impacts not only on agriculture but also on river flow and groundwater recharge. This analysis will exclude shorter-term events, which presents a certain limitation to the analysis. However, on a global level it allows for highlighting spatial patterns and differences between regions and as such provides useful information on the likely evolution of long-term droughts under different warming levels. To account of the fact that dealing with drought concepts in deserts, hyper-arid and cold areas might be physically meaningless and could lead to

unreliable results (Carrao et al., 2014; Spinoni et al., 2015b), we used the global aridity index dataset from Spinoni et al. (2015b) to exclude the deserts, hyper-arid and cold regions from the analysis.

The supply side of the water balance was derived directly from the precipitation simulated by the climate models. The methodology applied to estimate reference evapotranspiration (ETo) is relevant as discrepancies can propagate and have a significant effect when computing drought changes (van der Schrier *et al.*, 2011; Sheffield *et al.*, 2012). The use of simple evaporation formulae based only on temperature may overestimate drought trends with global warming when compared with more physically based methods that include a more comprehensive set of meteorological variables. ETo was therefore estimated here as the reference ET for a short crop with approximate height of 0.12m (similar to grass) based on the Penman-Monteith (P-M) equation. The P-M method uses daily minimum and maximum near-surface air temperature, near-surface specific humidity, surface air pressure, surface downwelling shortwave radiation, surface downwelling longwave radiation, and near-surface wind speed. Dewes et al. (2017) show that P-M provides a more physically robust treatment of ETo due to the sensitivity of the factors that are included in their formulation. Many features like regional patterns of inter-annual variability are well represented only when the different drivers like wind speed or humidity are included in the formulation of ETo. In that sense, Dewes et al. (2017) show that P-M is also the most appropriate estimation of ETo for climate projections and to be included in indices like the SPEI as the uncertainties that might be linked to the drivers (wind, humidity, etc.) are smaller than the uncertainties produced by other sources. ETo computations were performed at a daily time step with the LISVAP pre-processor of the distributed hydrological model LISFLOOD (van der Knijff *et al.*, 2010; Burek et al., 2013).

Accumulated water deficits over the 12 month aggregation period were converted into SPEI-12 standardized units by fitting a log-logistic distribution using an unbiased Probability Weighted Moments method (Vicente-Serrano & Beguería 2016). We then derive drought characteristics from the SPEI-12 series based on the truncation concept, which originates from the theory of runs (Mishra and Singh 2010). Following this approach, a drought event is defined as a period in which the drought indicator is below a certain threshold or truncation level. The drought characteristics considered here (see Table S2) are the run duration (length of event) and magnitude (cumulative deficit or the negative run sum). For the purpose of obtaining return values of the latter we fit a generalized Pareto distribution (GPD) by the method of moments through the deficit values of the selected drought events. To ensure sufficient events per 30-year time window (minimum of 5) and a stable estimation

of the GPD parameters, a threshold of -0.5 was applied to the SPEI-12 time series, which implies a negative deviation of at least 0.5 standard deviations in the SPEI-12 (representing an accumulation period of 12 months) to define the onset of a drought. Further, interdependency between events was minimized by imposing at least one season (3 months) as the independence time between two dry periods, whereas minor events that can distort the extreme value analysis were excluded by assuming a minimum drought event duration of 3 months (Engeland *et al.*, 2004; Feyen & Dankers 2009). Details on the estimation of the GPD parameters can be found in the supplementary material.

Return times are estimated using a peaks-over threshold model, in which the generalized Pareto distribution (GPD) is fitted to those data that exceed a specified level. Given certain distributional assumptions, the GPD is asymptotically optimal for the parametric modeling of threshold exceedances (Coles, 2001). In the case of droughts this applies to shortfalls or deficits below a low threshold. It was assumed that the drought deficit volumes corresponding to the shortfalls are independent and identically distributed. With the location parameter (or distribution origin) set to the lower bound (or threshold = -0.5) of the partial duration series, drought deficits for different recurrence intervals were then derived by inferring the scale (σ) and shape (ξ) parameters of the GP distribution in each pixel using the method of moments (Coles, 2001). This depends on the threshold used and is true when upper centiles are used but less clear for low centiles (e.g., Beguería, 2005). Moreover, differences in the obtained probabilities can be found for dry-spell series as a function of the chosen threshold (Vicente-Serrano & Beguería-Portugués, 2003). Details on the estimation and uncertainties of the GPD parameters can be found in the supplementary material. Optimally selected thresholds should provide the best return-time estimates for extremes at all levels; however, it is not necessary that they correspond to those deemed most relevant for impacts. A threshold of drought severity below -0.5 was selected to ensure a stable estimation and stationarity over each 30 year time-windows centered on each SWL. See the supplementary material for more details.

The ensemble mean changes in drought characteristics under different SWLs compared to the baseline were evaluated through the Mann-Whitney-Wilcoxon test (Storch & Zwiers 2003; Swain & Hayhoe 2015) and the corresponding p-value. This non-parametric test has the advantage of making no assumptions about the distribution of the data and was used to determine whether the mean values computed for the reference baseline and the specific warming levels are significantly different at a chosen level of significance.

3. Results

Figure S1 shows statistics of drought duration based on SPEI-12 in the baseline and under the SWLs considered for the regions defined in Figure S2. The distributions comprise duration values over all climate members and land pixels of the region, for which median and average durations are reported in Table S3. Over all global land surface pixels (excluding Antarctica), the average and median drought duration in the baseline is 7 months (Figure S8). There is some variability in drought length among regions, with droughts presently lasting longest in Oceania (12 months) while Northern Europe faces the shortest (5 months) drought events. The global median drought length is projected to slowly increase with warming from 8 months under 1.5°C warming to 9.5 months under 3°C warming. The global average drought length, however, shows a much more pronounced rise, to 9 and 11 months under 1.5°C and 2°C warming, respectively, which further climbs to 18 months when warming reaches 3°C. Apart from an increase in drought length for the majority of global land areas under warming, this implies a shift towards an increasingly positively skewed global distribution of drought length, with large variations in projected changes between regions and very strong increases in duration for some regions.

Northern Africa will experience the most dramatic rise in drought persistence. With median drought duration rising to prevail up to 20% of the time under 3°C of warming, drought conditions as defined for the baseline may become almost normal conditions here in a few decades if present rates of warming continue. Strong increases in drought length aggregated over regions are also projected for Western and Southern Africa, the Caribbean, Central America, Southern Europe and West Asia. In general, droughts are projected to shorten in length for most land areas north of latitude 55°N, as exemplified by the projected distributions for the Russian Federation, Northern Europe and North America. Due to the spatial extent of the latter and the strong reduction in drought length in Canada and southern Alaska, the strong rise in drought length projected for southern and central states of the US is masked. Similar strong rises in drought length for Australia, Iran, north-west China, Chile, Venezuela and the central and eastern regions of Brazil are offset by less strong or opposite changes in other parts of these macro-regions. Even though climate in Australia is mainly arid or semi-arid, the recent observed increases in precipitation and atmospheric evaporative demand in the west and decreases in the east depicted by Donohue et al. (2010) are in line with the observed changes presented in Figure 1. Donahue et al. (2010) found that the Penman formulation produced the most reasonable estimation of potential evaporation dynamics in Australia. In their work an attribution analysis was performed using the Penman formulation to quantify the contribution of each input variable to overall trends in potential evaporation. Whilst changes in air temperature were found to produce a large increase in Penman potential evaporation rates, changes in the other key variables each reduced the rates, resulting in an overall negative trend in Penman potential evaporation. This supports the premise that the greater the number of the four key variables that are incorporated in a

formulation, the more realistic the trends from that formulation become (Chen et al., 2005; Shenbin et al., 2006).

Spatial variations within macro-regions of projected droughts are better captured in Figure 1 that shows the global distribution of ensemble median drought magnitude in the baseline and changes therein under different levels of warming. Table S4 further lists the percentage of land fraction in each region that will experience a doubling and halving of drought magnitude. At present, drought magnitude is by far the largest in Australia, Eastern Africa, central Argentina and North-Eastern Brazil. Changes in drought magnitude and duration are strongly correlated and in the regions with increasing drought duration mentioned above, drought magnitudes are projected to rise rapidly with warming, with a doubling of drought magnitude in 30%, 38% and 51% of global land surface (excluding deserts, hyper-arid and cold regions) under 1.5, 2 and 3°C of warming, respectively. In most of Africa (except Equatorial Africa), Southern Europe, the Caribbean, Central America, West Asia and Australia accumulated water deficits could become more than 5-fold in size under 3°C of warming. In approximately 20% of the global land surface drought magnitude will halve with warming to 1.5°C and higher levels. This is mainly in the Russian Federation, southern Alaska and Canada, Northern Europe, but also parts of South-America, Eastern and South-eastern Asia.

Figure 2 shows for each macro-region the median projected frequency (over all cells and climate members) under the different warming levels (vertical axis) of baseline drought magnitude return values (horizontal axis). Increasing (decreasing) drought recurrence is denoted by lines under (above) the identity line, the climate ensemble median absolute deviation (shaded areas) describes the climate inter-model spread uncertainty. The corresponding spatial pattern of changes in the frequency of the present 50 year drought magnitude is presented in Figure 3. In regions with a strong increase in drought magnitude, events that are now considered very extreme show a rapid increase in drought occurrence with warming. More than 15% of global land could be exposed to a baseline 100-year drought event every 5 years under 3°C of global warming. For most of Africa, aside the zone around the equator, but also the Caribbean, Central America, Central and West Asia, Oceania and north-west China, droughts are projected to happen 5 to 10 times more frequent even under ambitious mitigation targets. Strong rises in recurrence frequency with warming are further projected for Southern Europe, large parts of Western and Eastern Europe, southern and central US, Chile, as well as central and eastern regions of Brazil. Regions with a reduction in drought magnitudes show an opposite tendency with a reduction in drought frequency.

4. Discussion and Conclusions

With increasing levels of warming more heat is added to the climate system. This induces changes in evaporative demand and precipitation that are shown to follow the Clausius-Clapeyron (C-C) scaling

(Scheff & Frierson 2014). Even though, there is still an open debate on the validity of the C-C law (e.g. Vicente-Serrano et al., 2017) most climate models project an increase in global precipitation of 1-3% per °C of global warming, although this value shows pronounced spatial variability (Liu *et al.*, 2013), with the global average precipitation constrained by the atmospheric radiative energy balance (Held & Soden 2006). Potential Evapotranspiration (PET), on the other hand, is predicted to increase by 1.5%-4% per °C warming (Scheff & Frierson 2014). This is confirmed by the progressive increase in ETo with warming that is projected with high confidence for all macro-regions (Figure S9). This implies that in the absence of a significant precipitation increase, this scenario leads to a general increase of drought conditions, as the drying of the surface is enhanced with water scarcity. However, regional changes in ETo depend also on the expected trends in other variables such as solar radiation, humidity and wind speed, which may diminish or exacerbate the role of temperature.

Projected changes in precipitation exhibit substantial spatial variation (Figure S9), with increases for most mid- and high-latitude land masses and decreases over mid-latitude and subtropical arid and semi-arid regions. For many regions uncertainty in precipitation projections remains high (Carrão *et al.*, 2017), particularly at higher levels of warming. There are few zones where the supply of water outweighs continental drying and the water balance will not progressively decline, like Northern Europe, South-eastern South America, Central Africa, Canada, the Russian Federation and China (except the north-west).

There is further evidence of warming-induced changes in circulation patterns and large-scale convective organization that might contribute to the extension of areas experiencing droughts. Since two years, the Greater Horn of Africa grapples with the worst drought in decades, affecting millions of people. It is linked to the strong El Niño of 2015-2016, which could double in frequency owing to global warming (Cai *et al.*, 2014). This increase in El Niño frequency results from warming surface waters over the eastern equatorial Pacific that occurs faster than in the surrounding ocean waters (Xie *et al.*, 2010), which drastically affects convection patterns and the development of severe droughts in drought prone areas such as Eastern and Southern Australia, North Eastern South America, India and Southern Africa (Davey *et al.*, 2014; Ashcroft *et al.*, 2016).

Other possible changes in large-scale atmospheric circulation that affect moisture regimes have been discussed in the literature. For instance, the seasonal migration of the intertropical convergence zone (ITCZ) and the locations of the large-scale subtropical dry zones and of the major tropical and subtropical deserts are projected to expand poleward due to the extension of the Hadley cell (Lu *et al.*, 2007). This in turn causes a drying tendency on the poleward flanks of the subtropics due to the expansion of the descending branch of the Hadley Cell, while the mid-latitude meridional circulation

cell moves poleward, shifting the main storm tracks towards the poles (Seager *et al.*, 2010). Subtropical drying and poleward moistening are also enhanced by an increase in poleward moisture transport by transient eddies, which to a certain extent implies that evaporated moisture diverges from the anticyclonic to the cyclonic regions (Held & Soden 2006, Chou *et al.*, 2009).

As a result of these warming induced changes in moisture supply and demand, approximately 2/3 of the world population will experience progressively longer and more frequent droughts for increasing warming levels. Global mean drought length is projected to progressively increase with warming, with a rate of 2.0 months/°C until reaching 1.5°C and then rapidly accelerating to up to 4.2 months/°C when approaching 3°C of global warming. This acceleration in drought duration could lead to more frequent mega-droughts (a decade-scale drought) only few times observed in the past, like the dust bowl in the United States (Fye *et al.*, 2003), the persistent drought in the Sahel (Folland *et al.*, 1986) or the recent "Millennium Drought" in southeast Australia depicted as the worst drought on the records (van Dijk *et al.*, 2013). Ault *et al.* (2014) show that in the U.S. Southwest the risk of a decade-scale mega-drought in the coming century is at least 80%, and could be higher than 90% in certain areas. There is evidence of recurrent mega-droughts reconstructed from paleoclimate data over north-central Europe in the last millennium (Cook *et al.*, 2015), which reinforce other evidence from North America (Cook *et al.*, 2014) and Asia (Cook *et al.*, 2010) that droughts were more severe, extensive, and prolonged over Northern Hemisphere land areas before the 20th century.

Elevated CO_2 (eCO_2) might partially offset the ecological effects of droughts by allowing plants to adapt even with less canopy conductance and lower levels of soil moisture available (Swann et al., 2016; Betts et al., 2007). The models included in the present analysis do not consider the impact of CO_2 fertilization, therefore the drought changes might be less intense if considering this effect. However, the level of uncertainties in representing the effects of eCO_2 is still high to draw conclusive results in a global analysis. For instance, there is no evidence of long-term eCO2 effects on hydrological partitioning in tropical rainforest catchments (Yang et al., 2016).

The main impact of long lasting droughts is linked to the lowering of groundwater and surface water reservoir levels that may temporary buffer demand under dry conditions. The projected strong lengthening of droughts will impede replenishment of water supplies and may result in a difficult recovery after the drought and long-term socio-economic impacts for any specific region (for instance, Diffenbaugh *et al.*, 2015). The strong increase in frequency of droughts may further pose considerable challenges for the design of water resource systems in many regions of the world to cope with more frequent periods of reduced water availability.

Acknowledgments

The research leading to these results has received funding from the European Union Seventh Framework Programme FP7/2007-2013 under grant agreement no 603864 (HELIX: High-End cLimate Impacts and eXtremes; www.helixclimate.eu). The EC-EARTH3-HR simulations were performed on resources provided by the Swedish National Infrastructure for Computing (SNIC) at PDC. The data used are listed in the references and their supporting material. Global SPEI projections are available for download at the url http://data.europa.eu/89h/jrc-climate-spei-drought-helix-ec-earth-1975-2100

References

Alfieri, L., Bisselink, B., Dottori, F., Naumann, G., de Roo, A., Salamon, P., Wyser, K. & Feyen, L. (2017). Global projections of river flood risk in a warmer world. *Earth's Future*, doi:10.1002/2016EF000485

Alfieri, L., Dottori, F., Betts, R., Salamon, P., & Feyen, L. (2018). Multi-Model Projections of River Flood Risk in Europe under Global Warming. *Climate*, 6(1), 6. doi:10.3390/cli6010006

Ault, T. R., Cole, J. E., Overpeck, J. T., Pederson, G. T., & Meko, D. M. (2014). Assessing the risk of persistent drought using climate model simulations and paleoclimate data. *Journal of Climate*, 27(20), 7529-7549.

Ashcroft, L., Gergis, J., & Karoly, D. J. (2016). Long-term stationarity of El Niño–Southern Oscillation teleconnections in southeastern Australia. *Climate Dynamics*, 46(9-10), 2991-3006.

Bachmair, S., Svensson, C., Hannaford, J., Barker, L. J., & Stahl, K. (2016). A quantitative analysis to objectively appraise drought indicators and model drought impacts. *Hydrol. Earth Syst. Sci.*, 20, 2589-2609, doi:10.5194/hess-20-2589-2016

Beguería, S. (2005). Uncertainties in partial duration series modelling of extremes related to the choice of the threshold value. *Journal of Hydrology*, 303(1), 215-230.

Beguería, S., Vicente-Serrano, S. M., Reig, F., & Latorre, B. (2014). Standardized precipitation evapotranspiration index (SPEI) revisited: Parameter fitting, evapotranspiration models, tools, datasets and drought monitoring. *Int. J. Climatol*, 34 (10), 3001-3023.

Betts, R. A., Boucher, O., Collins, M., Cox, P. M., Falloon, P. D., Gedney, N., Hemming, D. L., Huntingford, C., Jones, C. D., Sexton, D. M., & Webb, M. J. (2007). Projected increase in continental runoff due to plant responses to increasing carbon dioxide. *Nature*, 448 (7157) 1037-1041.

Blauhut, V., Stahl, K., Stagge, J. H., Tallaksen, L. M., De Stefano, L., & Vogt, J. (2016). Estimating drought risk across Europe from reported drought impacts, drought indices, and vulnerability factors. *Hydrol. Earth Syst. Sci*., 20, 2779-2800, doi:10.5194/hess-20-2779-2016

Burek, P., van der Knijff, J., & Ntegeka, V. (2013). LISVAP Evaporation Pre-Processor for the LISFLOOD Water Balance and Flood Simulation Model, User Manual. *EUR 26167 EN, Publication Office of the European Union, Luxembourg. doi:10.2788/26000*

Burke, E. J., & Brown, S. J., (2008). Evaluating uncertainties in the projection of future drought. *Journal of Hydrometeorology*, 9(2), 292-299.

Cai, W., Borlace, S., Lengaigne, M., Van Rensch, P., Collins, M., Vecchi, G., Timmermann, A., Santoso, A., McPhaden, M., Wu, L., England, M. H., Wang, G., Guilyardi, E. & Jin, F. (2014). Increasing frequency of extreme El Niño events due to greenhouse warming. *Nature climate change*, 4(2), 111-116.

Cannon, A. J., Sobie, S. R., & Murdock, T. Q. (2015). Bias correction of GCM precipitation by quantile mapping: How well do methods preserve changes in quantiles and extremes? *Journal of Climate*, 28 (17), 6938-6959.

Carrão, H., Singleton, A., Naumann, G., Barbosa, P., & Vogt, J. V. (2014). An optimized system for the classification of meteorological drought intensity with applications in drought frequency analysis. *Journal of Applied Meteorology and Climatology*, 53(8), 1943-1960.

Carrão, H., Naumann, G., & Barbosa, P., (2017). Global projections of drought hazard in a warming climate: a prime for disaster risk management. *Climate Dynamics* doi: 10.1007/s00382-017-3740-8

Chen, D., Gao, G., Xu, C.Y., Guo, J., & Ren, G. (2005). Comparison of the Thornthwaite method and pan data with the standard Penman–Monteith estimates of reference evapotranspiration in China. *Climate Research*, 28 (2), 123–132.

Chou, C., Neelin, J. D., Chen, C. A., & Tu, J. Y. (2009). Evaluating the "rich-get-richer" mechanism in tropical precipitation change under global warming. *Journal of Climate* 22(8), 1982-2005.

Coles, S. (2001). An Introduction to Statistical Modelling of Extreme Values. *Springer Series in Statistics. London.*

Cook, E. R., Seager, R., Kushnir, Y., Briffa, K. R., Büntgen, U., Frank, D., & Baillie, M (2015). Old World megadroughts and pluvials during the Common Era. *Science advances, 1(10), e1500561.*

Cook, B. I., Smerdon, J. E., Seager, R., & Cook, E. R., (2014). Pan-continental droughts in North America over the last millennium. *Journal of Climate, 27(1), 383-397.*

Cook, B. I., Smerdon, J. E., Seager, R., & Coats, S. (2014). Global warming and 21st century drying. *Climate Dynamics*, 43(9-10), 2607-2627.

Cook, E. R., Anchukaitis, K. J., Buckley, B. M., D'Arrigo, R. D., Jacoby, G. C., & Wright, W., (2010). Asian monsoon failure and megadrought during the last millennium. *Science, 328(5977) 486-489.*

Dai, A. (2013) Increasing drought under global warming in observations and models. *Nature Climate Change*, 3 (1), 52-58.

Davey, M. K., Brookshaw, A., & Ineson, S. (2014). The probability of the impact of ENSO on precipitation and near-surface temperature. *Climate Risk Management*, 1, 5-24.

De Kauwe, M. G., Medlyn, B. E., Zaehle, S., Walker, A. P., Dietze, M. C., Hickler, T., Jain, A. K., Luo, Y., Parton, W. J., Prentice, I. C., Smith, B., Thornton, P. E., Wang, S., Wang, Y., Wårlind, D., Weng, E., Crous, K. Y., Ellsworth, D. S, Hanson, P. J., Seok Kim, H., Warren, J. M., Oren, R., & Norby, R. J. (2013). Forest water use and water use efficiency at elevated CO_2: A model-data intercomparison at two contrasting temperate forest FACE sites. *Global Change Biology*, 19 (6), 1759-1779.

Demory, M. E., Vidale, P. L., Roberts, M. J., Berrisford, P., Strachan, J., Schiemann, R., & Mizielinski, M. S. (2014). The role of horizontal resolution in simulating drivers of the global hydrological cycle. *Climate Dynamics*, 42(7-8), 2201-2225.

Dewes, C. F., Rangwala, I., Barsugli, J. J., Hobbins, M. T., & Kumar, S. (2017). Drought risk assessment under climate change is sensitive to methodological choices for the estimation of evaporative demand. *PloS one*, 12(3), e0174045.

Diffenbaugh, N. S., Swain, D. L., Touma, D., (2015). Anthropogenic warming has increased drought risk in California. *Proceedings of the National Academy of Sciences*, 112(13), 3931-3936

Donohue, R. J., McVicar, T. R., & Roderick, M. L. (2010). Assessing the ability of potential evaporation formulations to capture the dynamics in evaporative demand within a changing climate. *Journal of Hydrology*, 386(1), 186-197.

Donohue, R. J., Roderick, M. L., McVicar, T. R., & Yang, Y. (2017). A simple hypothesis of how leaf and canopy-level transpiration and assimilation respond to elevated CO_2 reveals distinct response patterns between disturbed and undisturbed vegetation. *Journal of Geophysical Research: Biogeosciences*, 122 (1), 168-184.

Ehret, U., E. Zehe, V. Wulfmeyer, K. Warrach-Sagi & J. Liebert (2012). HESS Opinions "Should we apply bias correction to global and regional climate model data?," *Hydrol Earth Syst Sci*, 16(9), 3391–3404, doi:10.5194/hess-16-3391-2012

Engeland, K., Hisdal, H. & Frigessi A. (2004). Practical extreme value modelling of hydrological floods and droughts: A case study. *Extremes*, 7, 5– 30, doi:10.1007/s10687-004-4727-5

Feng, S., Trnka, M., Hayes, M., & Zhang, Y. (2017). Why Do Different Drought Indices Show Distinct Future Drought Risk Outcomes in the US Great Plains?. *Journal of Climate*, 30(1), 265-278.

Feyen, L., & Dankers, R. (2009). Impact of global warming on streamflow drought in Europe. *J. Geophys. Res.*, 114, D17116, doi:10.1029/2008JD011438

Folland, C. K., Palmer, T. N., & Parker, D. E. (1986). Sahel rainfall and worldwide sea temperatures, 1901–85. *Nature*, 320, 602–607, doi:10.1038/320602a0

Forzieri, G., Feyen, L., Rojas, R., Flörke, M., Wimmer, F., & Bianchi, A. (2014). Ensemble projections of future streamflow droughts in Europe. *Hydrology and Earth System Sciences* 18(1), 85-108.

Fye, F. K., D. W. Stahle, & E. R. Cook (2003). Paleoclimatic analogs to twentieth-century moisture regimes across the United States. *Bull. Amer. Meteor. Soc*., 84, 901–909, doi: 10.1175/BAMS-84-7-901

Gates, W., et al., (1999). An overview of the results of the Atmospheric Model Intercomparison Project (AMIP I) *Bull. Amer. Meteor. Soc.* 80, 29–55.

GISTEMP Team, (2017). GISS Surface Temperature Analysis (GISTEMP). NASA Goddard Institute for Space Studies. Dataset accessed 2017-02-21 at https://data.giss.nasa.gov/gistemp/

Hazeleger, W., et al., (2012) EC-Earth V2.2: Description and validation of a new seamless earth system prediction model. *Clim. Dyn.*, 39(11), 2611–2629, doi:10.1007/s00382-011-1228-5

Held, I. M., & Soden, B. J. (2006). Robust responses of the hydrological cycle to global warming. *Journal of Climate*, 19(21), 5686-5699.

Huang, S., Krysanova, V., & Hattermann, F. F. (2014). Does bias correction increase reliability of flood projections under climate change? A case study of large rivers in Germany. *International Journal of Climatology*, 34(14), 3780-3800.

James, R., Washington, R., Schleussner, C-F., Rogelj, J. & Conway, D. (2017). Characterizing half-a-degree difference: a review of methods for identifying regional climate responses to global warming targets. *WIREs Clim Change*, 8: n/a, e457. doi:10.1002/wcc.457

Jones, D. A., W. Wang, W., & Fawcett R. (2009). High-quality spatial climate data-sets for Australia. *Australian Meteor. Ocean. J.*, 58, 233-248.

Liu, J., Wang, B., Cane, M. A., Yim, S. Y., & Lee, J. Y. (2013). Divergent global precipitation changes induced by natural versus anthropogenic forcing. *Nature*, 493(7434), 656-659.

Lu, J., Vecchi, G. A., & Reichler, T. (2007). Expansion of the Hadley cell under global warming. *Geophysical Research Letters*, 34(6)

Lloyd-Hughes, B. (2014). The impracticality of a universal drought definition. *Theoretical and applied climatology*, 117(3-4), 607-611.

Masih, I., Maskey, S., Mussá, F., & Trambauer, P. (2014). A review of droughts on the African continent: a geospatial and long-term perspective. Hydrology and Earth System Sciences, 18(9), 3635.

McKee, T., Doesken, J., & Kleist, J. (1993). The relationship of drought frequency and duration to time scales. *In Proceedings of Eighth Conference on Applied Climatology. American Meteorological Society: Anaheim, CA*; 179–184.

Maule, C. F., Mendlik, T., & Christensen, O. B. (2017). The effect of the pathway to a two degrees warmer world on the regional temperature change of Europe. *Climate Services*, 7, 3-11.

Mishra, A. K., & Singh, V. P. (2010). A review of drought concepts. *Journal of Hydrology*, 391(1), 202-216.

Mueller, B., & Seneviratne, S. I. (2014). Systematic land climate and evapotranspiration biases in CMIP5 simulations. *Geophysical research letters, 41(1), 128-134.*

Naumann, G., Spinoni, J., Vogt, J. V., and Barbosa, P. (2015). Assessment of drought damages and their uncertainties in Europe. *Environmental Research Letters*, 10(12), 124013.

Orlowsky, B. & Seneviratne, S. I. (2013). Elusive drought: uncertainty in observed trends and short- and long-term CMIP5 projections. *Hydrol. Earth Syst. Sci.*, 17, 1765–1781, doi:10.5194/hess-17-1765-2013

Palmer, W. C. (1965). Meteorological drought. *Tech. Rep. Weather Bur. Res. Pap. 45, U.S. Dep. of Commerce*, Washington, D. C.

Peterson, T. C., et al., (2013). Monitoring and understanding changes in heat waves, cold waves, floods and droughts in the United States: State of knowledge. *Bull. Am. Meteor. Soc.*, 94, 821-834.

Prudhomme, C., Giuntoli, I., Robinson, E. L., Clark, D. B., Arnell, N. W., Dankers, R., Fekete, B. M., Franssen, W., Gerten, D., Gosling, S. N., Hagemann, S., Hannah, D. M., Kim, H., Masaki, Y., Satoh, Y., Stacke, T., Wada, Y., & Wisser, D. (2014). Hydrological droughts in the 21st century,

hotspots and uncertainties from a global multimodel ensemble experiment. *Proc. Natl. Acad. Sci.*, 111, 3262–3267, doi:10.1073/pnas.1222473110

Raftery, A. E., Zimmer, A., Frierson, D. M., Startz, R., & Liu, P. (2017). Less than 2°C warming by 2100 unlikely. *Nature Climate Change*, doi:10.1038/nclimate3352

Scheff, J., & Frierson, D. M. (2014). Scaling potential evapotranspiration with greenhouse warming *Journal of Climate*, 27(4), 1539-1558.

Shenbin, C., Yunfeng, L., & Thomas, A. (2006). Climatic change on the Tibetan Plateau: potential evapotranspiration trends from 1961–2000. *Climatic Change* 76 (3–4), 291–319. doi:10.1007/s10584-006-9080-z.

Schewe, J. et al., (2014). Multimodel assessment of water scarcity under climate change. *Proc. Natl Acad. Sci. USA* 111 3245–3250

Seager, R., Naik, N., & Vecchi, G. A. (2010). Thermodynamic and dynamic mechanisms for large-scale changes in the hydrological cycle in response to global warming. *Journal of Climate*, 23(17), 4651-4668.

Seager, R., Hoerling, M., Schubert, S., Wang, H., B. Lyon, B., Kumar, A., Nakamura, J., & Henderson, N. (2015). Causes of the 2011–14 California drought. *Journal of Climate*, 28, 6997-7024.

Sepulcre-Canto, G., Horion, S., Singleton, A., Carrao, H., & Vogt, J. (2012). Development of a Combined Drought Indicator to detect agricultural drought in Europe. *Natural Hazards and Earth System Sciences*, 12(11), 3519-3531.

Sheffield, J., & Wood, E. F. (2008). Projected changes in drought occurrence under future global warming from multimodel, multi-scenario, IPCC AR4 simulations. *Clim Dyn* 31:79–105.

Sheffield, J., Wood, E. F., & Roderick, M. L. (2012). Little change in global drought over the past 60 years. *Nature*, 491 (7424), 435-438.

Spinoni J., Naumann G., Vogt J., Barbosa P. (2015a). European drought climatologies and trends based on a multi-indicator approach. *Global and Planetary Change*, 127, 50-57

Spinoni, J., Vogt, J., Naumann, G., Carrao, H., & Barbosa, P. (2015b). Towards identifying areas at climatological risk of desertification using the Köppen–Geiger classification and FAO aridity index. *International Journal of Climatology*, 35(9), 2210-2222.

Storch H. V., & Zwiers F. W. (2003). Statistical analysis in Climate Research. *Virtual publishing ed., Cambridge University Press*.

Swain S., & Hayhoe K. (2015). CMIP5 projected changes in spring and summer drought and wet conditions over North America. *Clim Dyn*, 44(9-10), 2737-2750.

Tallaksen L. M., & Van Lanen H. A. J. (2004). Hydrological drought: processes and estimation methods for streamflow and groundwater. *Developments in Water Science 48, Elsevier Science B.V., the Netherlands.*

Taylor I. H., Burke E, McColl L., Falloon P. D., Harris G. R., & McNeall D. (2013). The impact of climate mitigation on projections of future drought. *Hydrol Earth Syst Sci* 17:2339–2358. doi:10.5194/hess-17-2339-2013

Themeßl M. J., A. Gobiet, & G. Heinrich (2012). Empirical-statistical downscaling and error correction of regional climate models and its impact on the climate change signal. *Clim. Change*, 112(2), 449–468, doi:10.1007/s10584-011-0224-4

Trambauer P., Maskey S., Werner M., Pappenberger F., Van Beek L. P., & Uhlenbrook S. (2014). Identification and simulation of space–time variability of past hydrological drought events in the Limpopo River basin, southern Africa. *Hydrology and Earth System Sciences*, 18(8), 2925-2942.

Trenberth K. E., Dai A., Van Der Schrier G., Jones P. D., Barichivich J., Briffa K. R., & Sheffield J. (2014). Global warming and changes in drought. *Nature Climate Change*, 4 (1), 17-22.

Touma D., Ashfaq M., Nayak M. A., Kao S-C., & Diffenbaugh N. S. (2015). A multi-model and multi-index evaluation of drought characteristics in the 21st century. *Journal of Hydrology*, 526, 196-207.

Ukkola A. M., De Kauwe M. G., Pitman A. J., Best M. J., Abramowitz G., Haverd V., Decker M., & Haughton N. (2016). Land surface models systematically overestimate the intensity, duration and magnitude of seasonal-scale evaporative droughts. *Environmental Research Letters*, 11 (10), art. No. 104012.

UNEP (2016). The Emissions Gap Report 2016. *United Nations Environment Programme (UNEP)*, Nairobi.

van der Knijff J. M., J. Younis, & A. P. de Roo (2010). LISFLOOD: A GIS-based distributed model for river basin scale water balance and flood simulation. *Int J Geogr Inf Sci*, 24(2), 189–212.

van der Schrier G., Jones P. D., Briffa K. R. (2011). The sensitivity of the PDSI to the Thornthwaite and Penman-Monteith parameterizations for potential evapotranspiration. *J Geophys Res Atmos* 116:D03106. doi:10.1029/2010JD015001

van Dijk A. I. J., H. E. Beck, R. S. Crosbie, R. de Jeu, Y. Y. Liu, G. M. Podger, B. Timbal, & N. R. Viney (2013). The Millennium Drought in southeast Australia (2001–2009): Natural and human causes and implications for water resources, ecosystems, economy, and society. *Water Resour. Res.*, 49, doi:10.1002/wrcr.20123

Van Vuuren D. P., Edmonds J., Kainuma M., Riahi K., Thomson A., Hibbard K., Hurtt G., Kram T., Krey V., Lamarque J. F., Masui T., Meinshausen M., Nakicenovic N., Smith S., & Rose S. (2011). The representative concentration pathways: an overview. *Climatic change*, 109(1-2), 5.

Vicente-Serrano, S. M., Nieto, R., Gimeno, L., Azorin-Molina, C., Drumond, A., El Kenawy, A., Dominguez-Castro, F., Tomas-Burguera, M., & Peña-Gallardo, M. (2017). Recent changes of relative humidity: regional connection with land and ocean processes, *Earth Syst. Dynam. Discuss.*, https://doi.org/10.5194/esd-2017-43

Vicente-Serrano, S. M., Van der Schrier, G., Beguería, S., Azorin-Molina, C., & Lopez-Moreno, J. I. (2015). Contribution of precipitation and reference evapotranspiration to drought indices under different climates. Journal of Hydrology, 526, 42-54.

Vicente-Serrano S. M. et al., (2014). Evidence of increasing drought severity caused by temperature rise in southern Europe. *Environ. Res. Lett.* 9 044001.

Vicente-Serrano S. M., & Beguería S. (2016). Comment on 'Candidate distributions for climatological drought indices (SPI and SPEI)'by James H. Stagge et al. *International Journal of Climatology*, 36(4), 2120-2131.

Vicente-Serrano S. M., Beguería S., & López-Moreno J. I. (2010). A multiscalar drought index sensitive to global warming: The standardized precipitation evapotranspiration index. *J Clim*, 23 (7), 1696-1718.

Vicente- Serrano, S. M., & Beguería- Portugués, S. (2003). Estimating extreme dry- spell risk in the middle Ebro valley (northeastern Spain): a comparative analysis of partial duration series with a general Pareto distribution and annual maxima series with a Gumbel distribution. *International Journal of Climatology*, 23(9), 1103-1118

Wanders N., Wada Y., & Van Lanen, H. A. (2015). Global hydrological droughts in the 21st century under a changing hydrological regime. *Earth System Dynamics*, 6 (1), 1-15.

Wang Z., Li J., Lai C., Zeng Z., Zhong R., Chen X., Zhou X., & Wang M. (2017). Does drought in China show a significant decreasing trend from 1961 to 2009? *Science of the Total Environment*, 579, 314-324.

Warszawski L., Frieler K., Huber V., Piontek F., Serdeczny O., & Schewe, J. (2014). The inter-sectoral impact model intercomparison project (ISI–MIP): project framework. *Proceedings of the National Academy of Sciences*, 111(9), 3228-3232.

Weedon G. P., Balsamo G., Bellouin N., Gomes S., Best M., & Viterbo P. (2014). The WFDEI meteorological forcing data set: WATCH Forcing Data methodology applied to ERA-Interim reanalysis data. *Water Resources Research 50(9) 7505-7514.*

WMO, (2008). Manual on low flow estimation and prediction, *Operational Hydrology Report No. 50, WMO-No. 1029, 136 pp*

Xie S. P., Deser C., Vecchi G. A., Ma J., Teng H., & Wittenberg A., (2010). Global warming pattern formation: Sea surface temperature and rainfall. *J Clim* 23(4), 966-986.

Yang, Y., Donohue, R. J., McVicar, T. R., Roderick, M. L., & Beck, H. E. (2016). Long- term CO2 fertilization increases vegetation productivity and has little effect on hydrological partitioning in tropical rainforests. *Journal of Geophysical Research: Biogeosciences*, 121(8), 2125-2140.

Zhao T., & Dai A. (2015). The magnitude and causes of global drought changes in the 21st century under a low–moderate emissions scenario. *J Clim* 28:4490–4512.

Zhao T., & Dai A. (2016). Uncertainties in historical changes and future projections of drought. Part II: model-simulated historical and future drought changes. *Climatic Change*, 1-14. doi:10.1007/s10584-016-1742-x

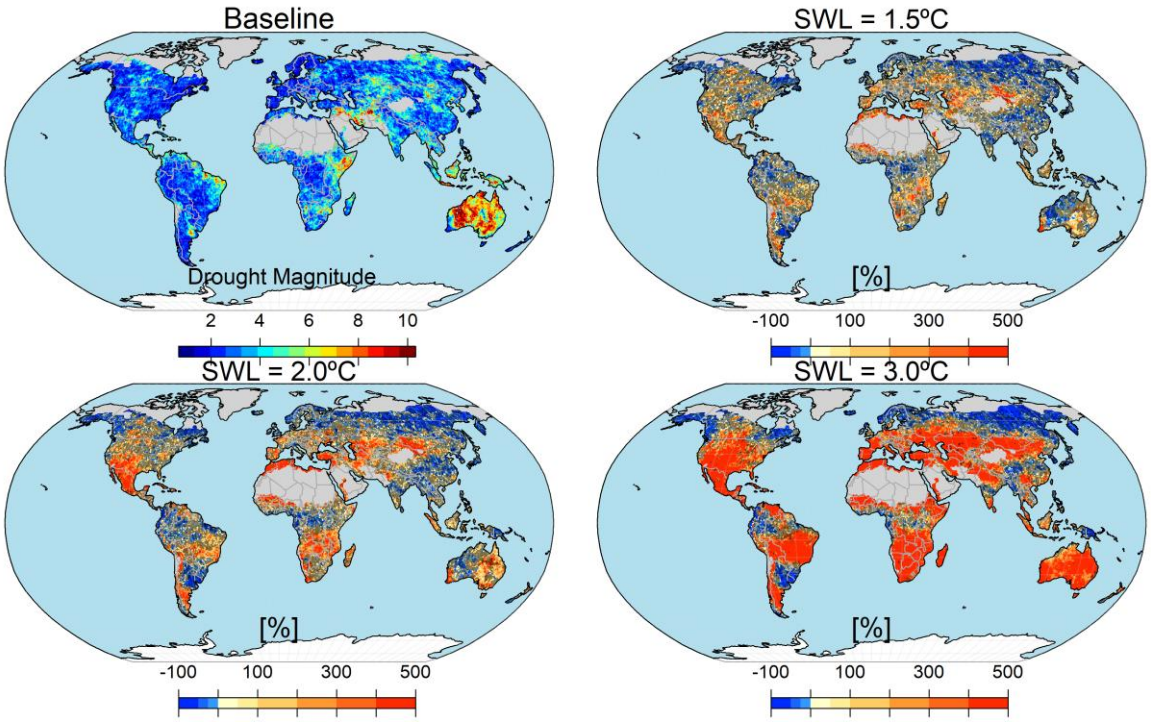

Figure 1. *Drought magnitude (upper-left plot) and relative changes [%] in drought magnitude with respect to the baseline for the three specific warming levels (1.5°C, 2.0°C, 3.0°C). Changes that are not statistically significant at the 10% level are shaded out in black. Territories excluded from the analysis are masked in grey.*

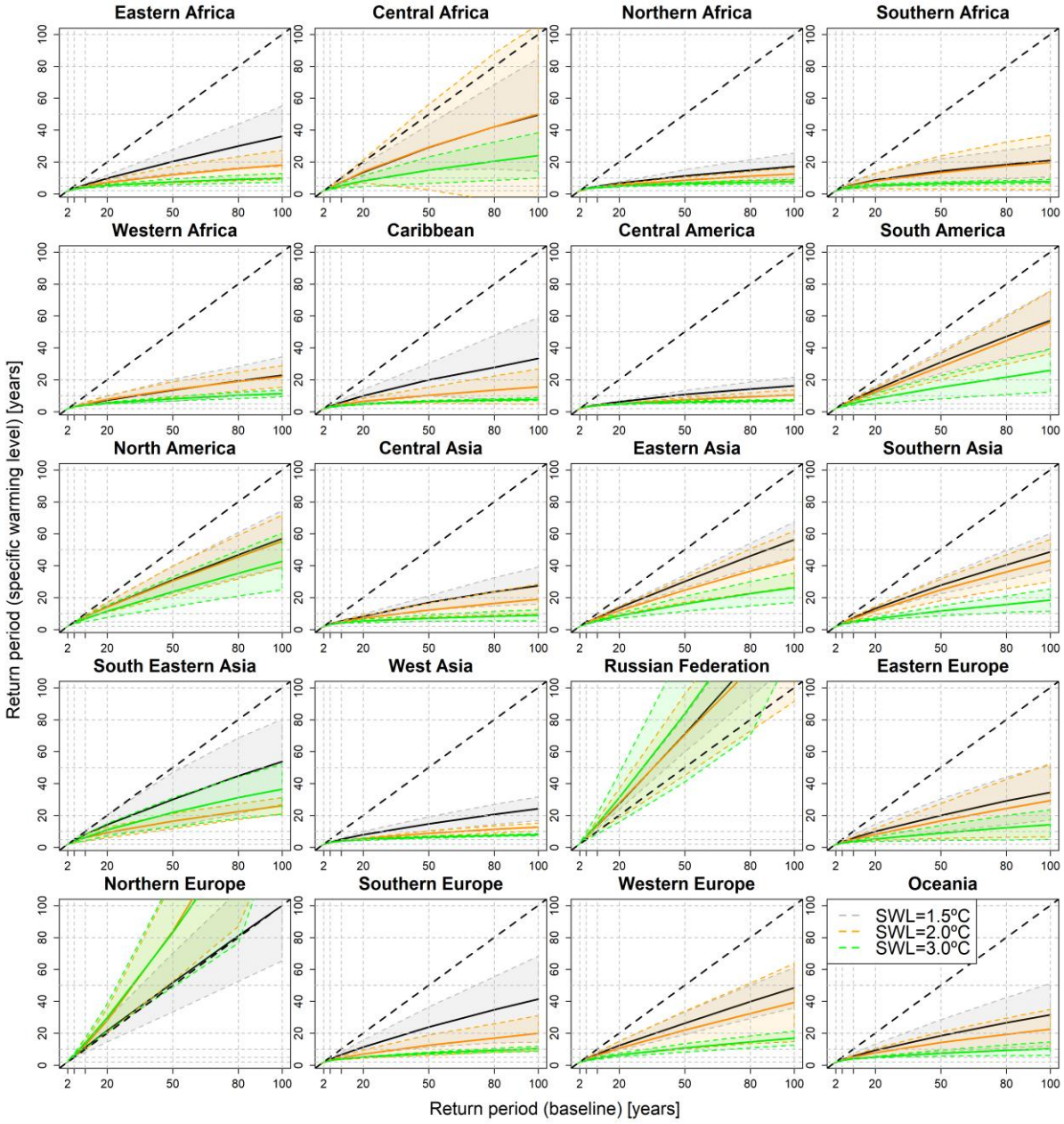

Figure 2. Changes in return periods of droughts in the different macro regions for 1.5°C (grey), 2°C (orange) and 3°C (green). Dashed black line represents the no-change curve and inter-model median absolute deviation (shaded areas).

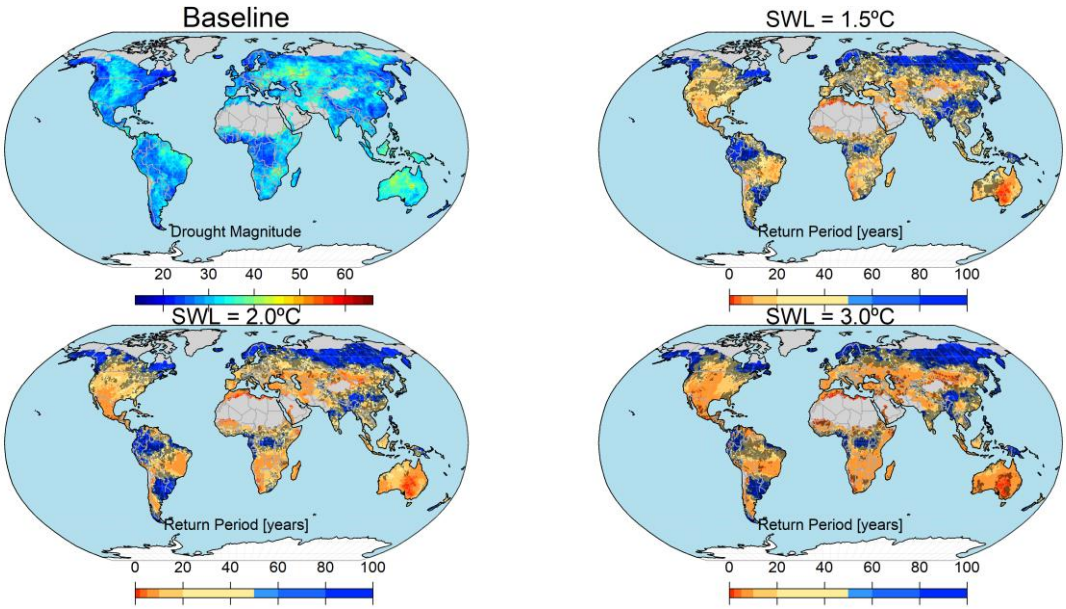

Figure 3. *Drought Magnit*ude for 50-yr return period droughts (baseline) and the *differences between return periods of 50-yr droughts for different warming levels (1.5°C, 2.0°C and 3.0° C). Changes that are not statistically significant at the 10% level are shaded out in black. Territories excluded from the analysis are masked in grey.*